

Magnetic moments of the spin- $\frac{3}{2}$ doubly heavy baryons

Lu Meng^{1,a}, Hao-Song Li^{1,b}, Zhan-Wei Liu^{2,c}, Shi-Lin Zhu^{1,3,d}

¹ School of Physics and State Key Laboratory of Nuclear Physics and Technology, Peking University, Beijing 100871, China

² School of Physical Science and Technology, Lanzhou University, Lanzhou 730000, China

³ Collaborative Innovation Center of Quantum Matter, Beijing 100871, China

Received: 28 October 2017 / Accepted: 2 December 2017 / Published online: 14 December 2017
© The Author(s) 2017. This article is an open access publication

Abstract In this work, we investigate the chiral corrections to the magnetic moments of the spin- $\frac{3}{2}$ doubly charmed baryons systematically up to next-to-next-to-leading order with the heavy baryon chiral perturbation theory. The numerical results are given up to next-to-leading order: $\mu_{\Xi_{cc}^{*++}} = 2.61\mu_N$, $\mu_{\Xi_{cc}^{*+}} = -0.18\mu_N$, $\mu_{\Omega_{cc}^{*+}} = 0.17\mu_N$. As a by-product, we have also calculated the magnetic moments of the spin- $\frac{3}{2}$ doubly bottom baryons and charmed bottom baryons: $\mu_{\Xi_{bb}^{*0}} = 2.83\mu_N$, $\mu_{\Xi_{bb}^{*-}} = -1.33\mu_N$, $\mu_{\Omega_{bb}^{*-}} = -1.54\mu_N$, $\mu_{\Xi_{bc}^{*+}} = 3.22\mu_N$, $\mu_{\Xi_{bc}^{*0}} = -0.84\mu_N$, $\mu_{\Omega_{bc}^{*0}} = -1.09\mu_N$.

1 Introduction

A doubly charmed baryon was first reported by the SELEX Collaboration in the decay model $\Xi_{cc}^+ \rightarrow \Lambda_c^+ K^- \pi^+$ with the mass $M_{\Xi_{cc}^+} = 3519 \pm 1 \text{ MeV}$ [1]. However, no other collaborations confirmed the observation [2–4]. Recently, the spin- $\frac{1}{2}$ doubly charmed baryon Ξ_{cc}^{++} was reported by the LHCb Collaboration in the $\Lambda_c^+ K^- \pi^+ \pi^+$ mass spectrum with the mass $M_{\Xi_{cc}^{++}} = 3621.40 \pm 0.72 \text{ (stat.)} \pm 0.27 \text{ (syst.)} \pm 0.14 \text{ (}\Lambda_c^+ \text{) MeV}$ [5].

The production of the doubly heavy baryons have been discussed in Refs. [6–14]. Apart from the spin- $\frac{1}{2}$ doubly charmed baryons, there exist the spin- $\frac{3}{2}$ doubly charmed baryons as degenerate states of the spin- $\frac{1}{2}$ ones in the heavy quark limit. In the past decades, the masses and other properties of spin- $\frac{1}{2}$ and spin- $\frac{3}{2}$ doubly charmed baryons have been investigated extensively in the literature [15–63], where the mass splittings between the spin- $\frac{1}{2}$ and spin- $\frac{3}{2}$ doubly charmed baryons are from several tens MeV to 100 MeV. Since the real or virtual photons are usually used as probes

to explore the inner structures of baryons, the electromagnetic form factors of the doubly charmed baryons are very important. Especially the magnetic moments encode crucial information of their underlying structure. In Refs. [17, 39, 64–76], the magnetic moments of the spin- $\frac{1}{2}$ and spin- $\frac{3}{2}$ doubly charmed baryons have been investigated.

The magnetic moments of the spin- $\frac{3}{2}$ doubly charmed baryons were first investigated in the naive quark model by Lichtenberg [64]. After that, many authors have employed the quark model to calculate the spin- $\frac{3}{2}$ doubly charmed baryon magnetic moments [34, 39, 69]. Apart from the quark models, the magnetic moments of the spin- $\frac{3}{2}$ doubly charmed baryons have been predicted employing the effective quark mass and screened charge scheme in Ref. [67]. The magnetic moments of the spin- $\frac{3}{2}$ doubly charmed baryons have also been calculated in the MIT bag model [70, 71] and skyrmion model [73].

Compared with the quark model, the chiral perturbation theory (ChPT) [77, 78] provides a systematic framework to calculate the electromagnetic form factors of the baryons order by order. However, the baryon mass does not vanish in the chiral limit, which introduces another energy scale besides the $\Lambda_\chi = 4\pi f_\pi$. In order to employ ChPT in the baryon sector, the heavy baryon chiral perturbation theory (HBChPT) was proposed [79–82]. The magnetic moments of the octet, decuplet and spin- $\frac{1}{2}$ doubly charmed baryons have been calculated in the framework of HBChPT [76, 80, 83, 84]. The decuplet to octet and spin- $\frac{3}{2}$ to spin- $\frac{1}{2}$ doubly charmed baryons transition magnetic moments were also investigated [79, 85–90].

In this paper, we investigate the magnetic moments of the spin- $\frac{3}{2}$ doubly heavy baryons within the framework of HBChPT. We use the quark model to estimate the low energy constants (LECs), since there does not exist any experiment data. The numerical results are given to the next-to-leading order while the analytical results are presented to the next-to-next-to-leading order.

^a e-mail: lmeng@pku.edu.cn

^b e-mail: haosongli@pku.edu.cn

^c e-mail: liuzhanwei@lzu.edu.cn

^d e-mail: zhusl@pku.edu.cn

We first discuss the electromagnetic form factors of the spin- $\frac{3}{2}$ baryons in Sect. 2. The chiral Lagrangians are constructed in Sect. 3. In Sect. 4, we calculate the magnetic moments analytically order by order. In Sect. 5, with the help of the quark model, we estimate the LECs and give the numerical results of the magnetic moments to the next-to-leading order. A short summary is given in Sect. 6. All the coefficients of the loop corrections are collected in Appendix A.

2 Electromagnetic form factors of the spin- $\frac{3}{2}$ doubly charmed baryons

For the spin- $\frac{3}{2}$ doubly charmed baryons, one can parameterize the general electromagnetic current matrix elements [91], which satisfy the gauge invariance, parity conservation and time-reversal invariance:

$$\langle T(p') | J_\mu | T(p) \rangle = \bar{u}^\rho(p') \mathcal{O}_{\rho\mu\sigma}(p', p) u^\sigma(p), \tag{1}$$

with

$$\begin{aligned} \mathcal{O}_{\rho\mu\sigma}(p', p) = & g_{\rho\sigma} \left(A_1 \gamma_\mu + \frac{A_2}{2M_T} P_\mu \right) \\ & + \frac{q_\rho q_\sigma}{(2M_T)^2} \left(C_1 \gamma_\mu + \frac{C_2}{2M_T} P_\mu \right), \end{aligned} \tag{2}$$

where p and p' are the momenta of the spin- $\frac{3}{2}$ doubly charmed baryons. $P = p + p'$, $q = p' - p$. M_T is the doubly charmed baryon mass and u_σ is the Rarita–Schwinger spinor [92].

In the heavy baryon limit, the baryon field can be decomposed into the large component \mathcal{T} and small component \mathcal{H} ,

$$T = e^{-iM_T v \cdot x} (\mathcal{T} + \mathcal{H}),$$

$$\mathcal{T} = e^{iM_T v \cdot x} \frac{1 + \not{v}}{2} T,$$

$$\mathcal{H} = e^{iM_T v \cdot x} \frac{1 - \not{v}}{2} T,$$

where v_μ is the velocity of the baryon. In the heavy baryon limit, the matrix elements of the electromagnetic current J_μ can be re-parametrized as [84]

$$\langle T(p') | J_\mu | T(p) \rangle = \bar{u}^\rho(p') \mathcal{O}_{\rho\mu\sigma}(p', p) u^\sigma(p), \tag{3}$$

with

$$\begin{aligned} \mathcal{O}_{\rho\mu\sigma}(p', p) = & g_{\rho\sigma} \left[v_\mu F_1(q^2) + \frac{[S_\mu, S_\alpha]}{M_T} q^\alpha F_2(q^2) \right] \\ & + \frac{q^\rho q^\sigma}{(2M_T)^2} \left[v_\mu F_3(q^2) + \frac{[S_\mu, S_\alpha]}{M_T} q^\alpha F_4(q^2) \right] \end{aligned} \tag{4}$$

where $S_\mu = \frac{i}{2} \gamma_5 \sigma_{\mu\nu} v^\nu$ is the covariant spin-operator. The charge (E0), electro-quadrupole (E2), magnetic-dipole (M1), and magnetic octupole (M3) form factors read

$$\begin{aligned} G_{E0}(q^2) = & \left(1 + \frac{2}{3} \tau \right) [F_1 + \tau(F_1 - F_2)] \\ & - \frac{1}{3} \tau(1 + \tau) [F_3 + \tau(F_3 - F_4)], \end{aligned} \tag{5}$$

$$\begin{aligned} G_{E2}(q^2) = & [F_1 + \tau(F_1 - F_2)] \\ & - \frac{1}{2} (1 + \tau) [F_3 + \tau(F_3 - F_4)], \end{aligned} \tag{6}$$

$$G_{M1}(q^2) = \left(1 + \frac{4}{5} \tau \right) F_2 - \frac{2}{5} \tau(1 + \tau) F_4, \tag{7}$$

$$G_{M3}(q^2) = F_2 - \frac{1}{2} (1 + \tau) F_4. \tag{8}$$

where $\tau = -\frac{q^2}{(2M_T)^2}$. When $q^2 = 0$, we obtain the magnetic moment $\mu_T = G_{M1}(0) \frac{e}{2M_T}$.

3 Chiral Lagrangians

3.1 The leading order chiral Lagrangians

To calculate the chiral corrections to the magnetic moments, we construct the relevant chiral Lagrangians. The doubly charmed baryon fields read

$$B = \begin{pmatrix} \Xi_{cc}^{++} \\ \Xi_{cc}^+ \\ \Omega_{cc}^+ \end{pmatrix}, \quad T^\mu = \begin{pmatrix} \Xi_{cc}^{*++} \\ \Xi_{cc}^{*+} \\ \Omega_{cc}^{*+} \end{pmatrix}^\mu, \quad \Rightarrow \begin{pmatrix} ccu \\ ccd \\ ccs \end{pmatrix}, \tag{9}$$

where B and T^μ are spin- $\frac{1}{2}$ and spin- $\frac{3}{2}$ doubly charmed baryon fields, respectively. We follow the notations in Refs. [78, 82, 84] to define the basic chiral effective Lagrangians of the pseudoscalar mesons. The pseudoscalar meson fields are introduced as follows:

$$\phi = \begin{pmatrix} \pi^0 + \frac{1}{\sqrt{3}} \eta & \sqrt{2} \pi^+ & \sqrt{2} K^+ \\ \sqrt{2} \pi^- & -\pi^0 + \frac{1}{\sqrt{3}} \eta & \sqrt{2} K^0 \\ \sqrt{2} K^- & \sqrt{2} \bar{K}^0 & -\frac{2}{\sqrt{3}} \eta \end{pmatrix}. \tag{10}$$

The chiral connection and axial vector field are defined as [78, 82],

$$\Gamma_\mu = \frac{1}{2} [u^\dagger (\partial_\mu - i r_\mu) u + u (\partial_\mu - i l_\mu) u^\dagger], \tag{11}$$

$$u_\mu = i [u^\dagger (\partial_\mu - i r_\mu) u - u (\partial_\mu - i l_\mu) u^\dagger], \tag{12}$$

where

$$u^2 = U = \exp(i\phi/f_0) \tag{13}$$

$$r_\mu = l_\mu = -eQA_\mu. \tag{14}$$

For the Lagrangians with the baryon fields, $Q = Q_B = \text{diag}(2, 1, 1)$ and for the pure meson Lagrangians $Q = Q_M = \text{diag}(2/3, -1/3, -1/3)$. f_0 is the decay constant of the pseudoscalar meson in the chiral limit. The experimental value of the pion decay constant $f_\pi \approx 92.4$ MeV while $f_K \approx 113$ MeV, $f_\eta \approx 116$ MeV.

The leading order ($\mathcal{O}(p^2)$) pure meson Lagrangian is

$$\mathcal{L}_{\pi\pi}^{(2)} = \frac{f_0^2}{4} \text{Tr}[\nabla_\mu U (\nabla^\mu U)^\dagger], \tag{15}$$

$$\nabla_\mu U = \partial_\mu U - ir_\mu U + iUl_\mu, \tag{16}$$

where the superscript denotes the chiral order. The leading order doubly charmed baryon Lagrangians and meson-baryon interaction Lagrangians read

$$\mathcal{L}_{TT}^{(1)} = \bar{T}^\mu [-g_{\mu\nu}(i\mathcal{D} - M_T) + i(\gamma_\mu D_\nu + \gamma_\nu D_\mu) - \gamma_\mu(i\mathcal{D} + M_T)\gamma_\nu]T^\nu + \frac{H}{2} (\bar{T}^\mu g_{\mu\nu} \not{u} \gamma_5 T^\nu), \tag{17}$$

$$\mathcal{L}_{BB}^{(1)} = \bar{B}(i\mathcal{D} - M_B + \frac{\tilde{g}_A}{2} \gamma^\mu \gamma_5 u_\mu)B, \tag{18}$$

$$\mathcal{L}_{BT}^{(1)} = \frac{C}{2} (\bar{T}^\mu u_\mu B + \bar{B}u_\mu T^\mu). \tag{19}$$

We use the subscript to denote the two particles involved in the Lagrangians. M_B is the spin- $\frac{1}{2}$ doubly charmed baryon mass. \tilde{g}_A , C and H are the coupling constants. The covariant derivative is defined as $D_\mu \equiv \partial_\mu + \Gamma_\mu$. Both \mathcal{L}_{TT} and \mathcal{L}_{BB} contain the free and interaction terms.

In the framework of HBChPT, the leading order non-relativistic Lagrangians read

$$\mathcal{L}_{TT}^{(1)} = \bar{T}^\mu [-iv \cdot D g_{\mu\nu}]T^\nu + H(\bar{T}^\mu g_{\mu\nu} u \cdot S T^\nu), \tag{20}$$

$$\mathcal{L}_{BT}^{(1)} = \frac{C}{2} (\bar{T}^\mu u_\mu B + \bar{B}u_\mu T^\mu), \tag{21}$$

$$\mathcal{L}_{BB}^{(1)} = \bar{B}i(v \cdot D - \delta)B + \bar{B}\tilde{g}_A S \cdot uB, \tag{22}$$

where $\delta \equiv M_B - M_T$. Since the spin- $\frac{3}{2}$ doubly charmed baryons have not been observed in the experiments, we take two values for the mass splitting, $\delta = -100$ MeV and $\delta = -70$ MeV, in our work. We do not consider the mass difference among the doubly charmed baryon triplets. The coupling constants are estimated with the help of the quark model in Refs. [76,90], $\tilde{g}_A = -\frac{1}{5}g_N = -0.25$, $C = -\frac{2\sqrt{3}}{5}g_N = -0.88$ and $H = -\frac{3}{5}g_N = -0.76$, where $g_N = 1.267$ is the nucleon axial charge. For the pseudoscalar meson masses, we use $m_\pi = 0.140$ GeV, $m_K = 0.494$ GeV, and $m_\eta = 0.550$ GeV. We use the nucleon mass $M_N = 0.938$ GeV.

3.2 The next-to-leading order chiral Lagrangians

The $\mathcal{O}(p^2)$ Lagrangians contribute to the magnetic moments of the spin- $\frac{3}{2}$ doubly charmed baryons

$$\mathcal{L}_{TT}^{(2)} = \frac{-ib_1^{tt}}{2M_T} \bar{T}^\mu \hat{F}_{\mu\nu}^+ T^\nu + \frac{-ib_2^{tt}}{2M_T} \bar{T}^\mu \langle F_{\mu\nu}^+ \rangle T^\nu, \tag{23}$$

$$\mathcal{L}_{BB}^{(2)} = \frac{b_1^{bb}}{8M_T} \bar{B}\sigma^{\mu\nu} \hat{F}_{\mu\nu}^+ B + \frac{b_2^{bb}}{8M_T} \bar{B}\sigma^{\mu\nu} \langle F_{\mu\nu}^+ \rangle B, \tag{24}$$

$$\begin{aligned} \mathcal{L}_{BT}^{(2)} = & b_1^{bt} \frac{i}{4M_T} \bar{B} \hat{F}_{\mu\nu}^+ \gamma^\nu \gamma_5 T^\mu + b_2^{bt} \frac{i}{4M_T} \bar{B} \langle F_{\mu\nu}^+ \rangle \gamma^\nu \gamma_5 T^\mu \\ & - b_1^{bt} \frac{i}{4M_T} \bar{T}^\mu \hat{F}_{\mu\nu}^+ \gamma^\nu \gamma_5 B - b_2^{bt} \frac{i}{4M_T} \bar{T}^\mu \langle F_{\mu\nu}^+ \rangle \gamma^\nu \gamma_5 B, \end{aligned} \tag{25}$$

where the coefficients $b_{1,2}^{tt,bb,bt}$ are the LECs which contribute to the magnetic moments at tree level. The chiral covariant QED field strength tensors $F_{\mu\nu}^\pm$ are defined as

$$F_{\mu\nu}^\pm = u^\dagger F_{\mu\nu}^R u \pm u F_{\mu\nu}^L u^\dagger, \tag{26}$$

$$F_{\mu\nu}^R = \partial_\mu r_\nu - \partial_\nu r_\mu - i[r_\mu, r_\nu], \tag{27}$$

$$F_{\mu\nu}^L = \partial_\mu l_\nu - \partial_\nu l_\mu - i[l_\mu, l_\nu]. \tag{28}$$

Since Q_B is not traceless, the operator $F_{\mu\nu}^+$ can be divided into two parts, $\hat{F}_{\mu\nu}^+$ and $\langle F_{\mu\nu}^+ \rangle$. $\langle F_{\mu\nu}^+ \rangle \equiv \text{Tr}(F_{\mu\nu}^+)$. The operator $\hat{F}_{\mu\nu}^+ = F_{\mu\nu}^+ - \frac{1}{3}\langle F_{\mu\nu}^+ \rangle$ is traceless and transforms as the adjoint representation under the chiral transformation. Recall that for the direct product of the representation of the SU(3) group $3 \otimes \bar{3} = 1 \oplus 8$. Therefore, there are two independent interaction terms in the $\mathcal{O}(p^2)$ Lagrangians for the magnetic moments of the doubly charmed baryons. The non-relativistic Lagrangians corresponding to Eqs. (23)–(25) are

$$\mathcal{L}_{TT}^{(2)} = \frac{-ib_1^{tt}}{2M_T} \bar{T}^\mu \hat{F}_{\mu\nu}^+ T^\nu + \frac{-ib_2^{tt}}{2M_T} \bar{T}^\mu \langle F_{\mu\nu}^+ \rangle T^\nu, \tag{29}$$

$$\begin{aligned} \mathcal{L}_{BT}^{(2)} = & b_1^{bt} \frac{i}{2M_T} \bar{B} \hat{F}_{\mu\nu}^+ S^\nu T^\mu + b_2^{bt} \frac{i}{2M_T} \bar{B} \langle F_{\mu\nu}^+ \rangle S^\nu T^\mu \\ & - b_1^{bt} \frac{i}{2M_T} \bar{T}^\mu \hat{F}_{\mu\nu}^+ S^\nu B - b_2^{bt} \frac{i}{2M_T} \bar{T}^\mu \langle F_{\mu\nu}^+ \rangle S^\nu B, \end{aligned} \tag{30}$$

$$\mathcal{L}_{BB}^{(2)} = -\frac{ib_1^{bb}}{4M_T} \bar{B}[S^\mu, S^\nu] \hat{F}_{\mu\nu}^+ B - \bar{B} \frac{ib_2^{bb}}{4M_T} [S^\mu, S^\nu] \langle F_{\mu\nu}^+ \rangle B, \tag{31}$$

We also need the second order pseudoscalar meson and doubly charmed baryon interaction Lagrangians

$$\begin{aligned} \mathcal{L}_{TT}^{(2)} = & \frac{ig_1^{tt}}{4M_T} \bar{T}^\mu \{u_\rho, u_\sigma\} \sigma^{\rho\sigma} g_{\mu\nu} T^\nu \\ & + \frac{ig_2^{tt}}{4M_T} \bar{T}^\mu [u_\rho, u_\sigma] \sigma^{\rho\sigma} g_{\mu\nu} T^\nu, \end{aligned} \tag{32}$$

Table 1 The possible flavor structures of the $\mathcal{O}(p^4)$ Lagrangians which contribute to the magnetic moments

Group representation	$1 \otimes 1 \rightarrow 1$	$1 \otimes 8 \rightarrow 8$	$8 \otimes 1 \rightarrow 8$	$8 \otimes 8 \rightarrow 1$	$8 \otimes 8 \rightarrow 8_1$	$8 \otimes 8 \rightarrow 8_2$
Flavor structure	$\langle F_{\mu\nu}^+ \rangle \langle \chi_+ \rangle$	$\langle F_{\mu\nu}^+ \rangle \hat{\chi}_+$	$\hat{F}_{\mu\nu}^+ \langle \chi_+ \rangle$	$\langle \hat{F}_{\mu\nu}^+ \hat{\chi}_+ \rangle$	$[\hat{F}_{\mu\nu}^+, \hat{\chi}_+]$	$\{\hat{F}_{\mu\nu}^+, \hat{\chi}_+\}$

where $g_{1,2}^{tt}$ are the coupling constants. Recall that, for SU(3) group representations,

$$3 \otimes \bar{3} = 1 \oplus 8, \tag{33}$$

$$8 \otimes 8 = 1 \oplus 8_1 \oplus 8_2 \oplus 10 \oplus \bar{10} \oplus 27. \tag{34}$$

Both u_μ and u_ν transform as the adjoint representation. The two terms in Eq. (32) correspond to the product of u_μ and u_ν belonging to the 8_1 and 8_2 flavor representations, respectively. The g_1^{tt} term vanishes because of the anti-symmetric Lorentz structure. Thus, there is only one linearly independent LEC g_2^{tt} , which contributes to the spin- $\frac{3}{2}$ doubly charmed baryon magnetic moments up to $\mathcal{O}(p^3)$. The second order pseudoscalar meson and baryon non-relativistic Lagrangian reads

$$\mathcal{L}_{TT}^{(2)} = \frac{g_2^{tt}}{2M_T} \bar{T}^\mu [S^\rho, S^\sigma] [u_\rho, u_\sigma] g_{\mu\nu} T^\nu \tag{35}$$

The above Lagrangian contributes to the doubly charmed baryon magnetic moments in the diagram (j) of Fig. 2.

3.3 The higher order chiral Lagrangians

To calculate the $\mathcal{O}(p^3)$ magnetic moments at the tree level, we also need the $\mathcal{O}(p^4)$ electromagnetic chiral Lagrangians. The possible flavor structures are listed in Table 1, where $\chi^+ = \text{diag}(0, 0, 1)$ at the leading order. Recalling the flavor representation in Eqs. (33) and (34), the leading order term of the operator $[\hat{F}_{\mu\nu}^+, \hat{\chi}_+]$ vanishes after expansion since both $F_{\mu\nu}^+$ and χ^+ are diagonal. Meanwhile, the $\langle F_{\mu\nu}^+ \rangle \langle \chi_+ \rangle$ and $\langle F_{\mu\nu}^+ \rangle \hat{\chi}_+$ terms can be absorbed into Eq. (23) by renormalizing the LECs b_1^{tt} and b_2^{tt} . Thus, the independent $\mathcal{O}(p^4)$ Lagrangians read

$$\begin{aligned} \mathcal{L}^{(4)} = & \frac{-ia_1}{2M_T} \bar{T}^\mu \langle F_{\mu\nu}^+ \rangle \hat{\chi}_+ T^\nu + \frac{-ia_2}{2M_T} \bar{T}^\mu \langle \hat{F}_{\mu\nu}^+ \hat{\chi}_+ \rangle T^\nu \\ & + \frac{-ia_3}{2M_T} \bar{T}^\mu \{ \hat{F}_{\mu\nu}^+, \hat{\chi}_+ \} \hat{\chi}_+ T^\nu. \end{aligned} \tag{36}$$

4 Formalism up to one-loop level

We adopt the standard power counting scheme as in Refs. [93, 94]. The chiral order D_χ of a Feynman diagram is

$$D_\chi = 2L + 1 + \sum_d (d - 2) N_d^M + \sum_d (d - 1) N_d^{MB}, \tag{37}$$

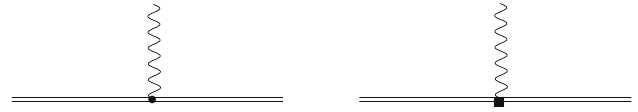


Fig. 1 The $\mathcal{O}(p^2)$ and $\mathcal{O}(p^4)$ tree level diagrams where the spin- $\frac{3}{2}$ doubly charmed baryon is denoted by the double solid line. The solid dot and black square represent the second- and fourth-order couplings, respectively

with L the number of loops and N_d^M, N_d^{MB} the number of d dimensional vertices from the meson and meson–baryon Lagrangians, respectively. The chiral order of the magnetic moment μ_T is $(D_\chi - 1)$.

The leading order ($\mathcal{O}(p^1)$) magnetic moments come from the tree diagram in Fig. 1 with the $\mathcal{O}(p^2)$ vertex. The magnetic moment is

$$\mu^{(1)} = -2\alpha \frac{M_N}{M_T} \mu_N \tag{38}$$

The μ_N is the nucleon magneton. α are the Clebsch–Gordan coefficients, which are collected in Table 6. Up to leading order, there are two unknown LECs, b_1^{tt} and b_2^{tt} .

There are four diagrams (a)–(d) which contribute to the next-to-leading order magnetic moments of the spin- $\frac{3}{2}$ doubly charmed baryons, as shown in Fig. 2. All the vertices in (a)–(d) come from Eqs. (15), (20) and (21). The diagrams (c) and (d) vanish in the heavy baryon mass limit. In particular, the amplitudes of the diagrams (c) and (d) are denoted \mathcal{M}_c and \mathcal{M}_d . We have

$$\begin{aligned} \mathcal{M}_c \propto & \int \frac{d^d l}{(2\pi)^d} \frac{i}{l^2 - m_\phi^2 + i\epsilon} \frac{(S \cdot l)}{f_0} \frac{-i P_{\rho\sigma}^{3/2}}{v \cdot l + i\epsilon} S_\mu \\ & \propto S \cdot v = 0, \end{aligned} \tag{39}$$

$$\begin{aligned} \mathcal{M}_d \propto & \int \frac{d^d l}{(2\pi)^d} \frac{i}{l^2 - m_\phi^2 + i\epsilon} \frac{l_\sigma}{f_0} \frac{i}{v \cdot l - \omega + i\epsilon} g_{\mu\rho} \\ & \propto g_{\mu\rho} v_\sigma, \end{aligned} \tag{40}$$

where $P_{\rho\sigma}^{3/2}$ is the non-relativistic spin- $\frac{3}{2}$ projector. \mathcal{M}_d vanishes since $v_\sigma u^\sigma = 0$. In other words, diagrams (c) and (d) do not contribute to the magnetic moments in the leading order of the heavy baryon expansion. The $\mathcal{O}(p^2)$ magnetic moment is

$$\mu^{(2)} = \sum_{\phi=\pi, K} (\mathcal{A}^\phi + \mathcal{B}^\phi) \beta_a^\phi, \tag{41}$$

$$\mathcal{A}^\phi = \frac{H^2 M_N m_\phi}{96 f_\phi^2} \mu_N, \tag{42}$$

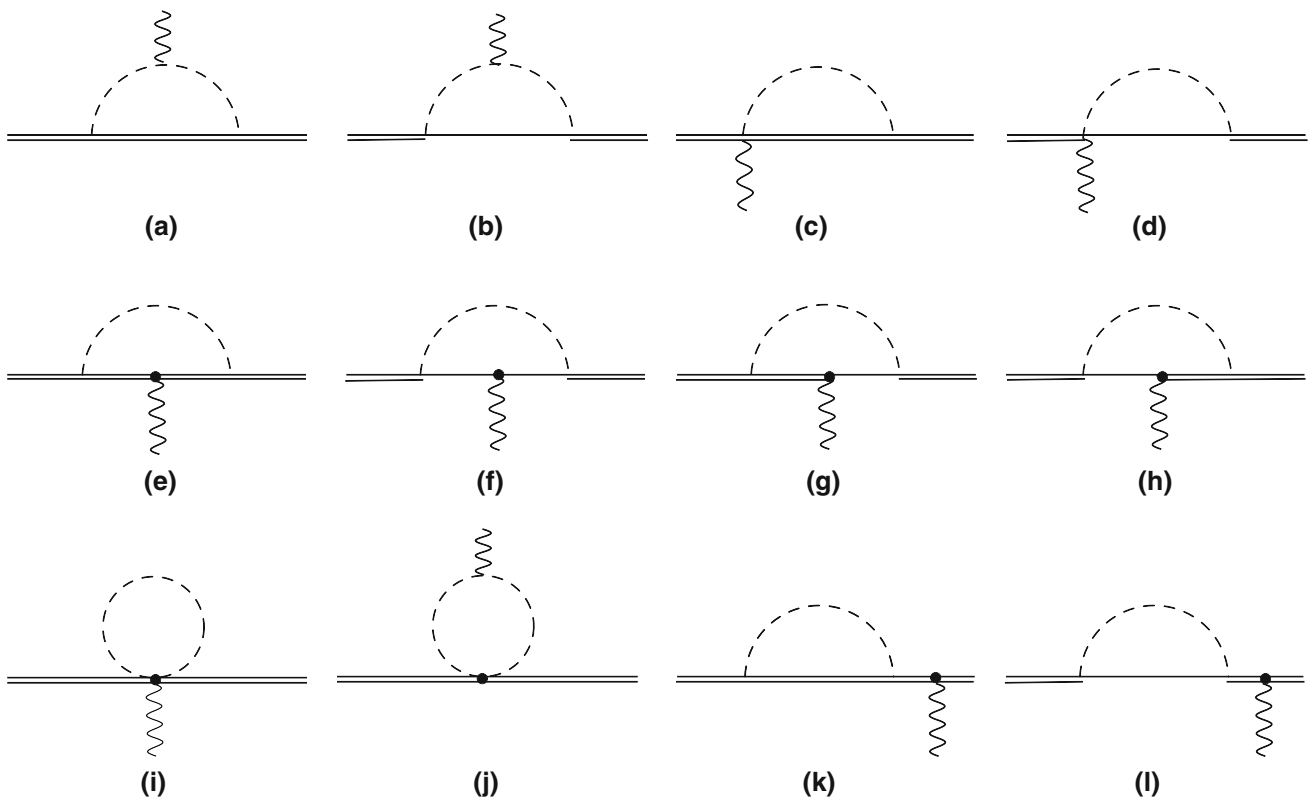


Fig. 2 The one-loop diagrams where the spin- $\frac{3}{2}$ (spin- $\frac{1}{2}$) doubly charmed baryon is denoted by the double (single) solid line. The dashed and wiggly lines represent the pseudoscalar meson and photon, respectively. The solid dots represent $\mathcal{O}(p^2)$ vertices, while the other vertices are at the leading order

$$\mathcal{B}^\phi = \frac{C^2 M_N \mu_N}{64\pi^2 f_\phi^2} \left[2\sqrt{m_\phi^2 - \delta^2} \arccos\left(\frac{\delta}{m_\phi}\right) - \delta \left(\ln \frac{m_\phi^2}{\lambda^2} - 1 \right) \right] \quad (43)$$

where β_a^ϕ are the Clebsch–Gordan coefficients, which are collected in Table 6. Up to $\mathcal{O}(p^2)$, there are five unknown LECs, $b''_{1,2}$, C , H and \tilde{g}_A . C , H and \tilde{g}_A can be estimated with the quark model.

There are eight loop diagrams (e)–(l) in Fig. 2, which contribute at $\mathcal{O}(p^3)$. For the (e)–(h) diagrams, the photon–baryon vertices are from the $\mathcal{O}(p^2)$ interaction terms in Eqs. (29)–(31), while the meson–baryon vertices are from Eqs. (20) and (21). The vertex in diagram (i) is from Eq. (29). The meson–baryon vertex in diagram (j) is from the Lagrangian in Eq. (32) while the meson–photon vertex is from the Lagrangian in Eq. (15). The loops (k) and (l) represent the wave function renormalization. The photon–baryon vertices are from the Lagrangians in Eq. (29), while the meson–baryon vertices are from the interaction in Eqs. (20) and (21). The contributions to the magnetic moments from the eight loop diagrams read

$$\begin{aligned} \mu_{\text{loop}}^{(3)} = & \sum_{\phi=\eta,\pi,K} (\mathcal{E}^\phi \gamma_e^\phi + \mathcal{F}^\phi \gamma_f^\phi + \mathcal{G}^\phi \gamma_g^\phi + \mathcal{H}^\phi \gamma_h^\phi) \\ & + \sum_{\phi=\pi,K} (\mathcal{I}^\phi \delta^\phi + \mathcal{J}^\phi \eta^\phi) + \sum_{\phi=\pi,\eta,K} (\mathcal{K}^\phi + \mathcal{L}^\phi) \xi^\phi \mu^{(1)} \end{aligned} \quad (44)$$

where

$$\mathcal{E}^\phi = -\frac{H^2 m_\phi^2}{864\pi^2 f_\phi^2} \frac{M_N}{M_T} \mu_N \left(33 \ln \frac{m_\phi^2}{\lambda^2} + 70 \right), \quad (45)$$

$$\begin{aligned} \mathcal{F}^\phi = & -\frac{C^2}{64\pi^2 f_\phi^2} \frac{M_N}{M_T} \mu_N \left[2\delta^2 + (m_\phi^2 - 2\delta^2) \ln \frac{m_\phi^2}{\lambda^2} \right. \\ & \left. + 4\delta \sqrt{m_\phi^2 - \delta^2} \arccos\left(\frac{\delta}{m_\phi}\right) \right], \end{aligned} \quad (46)$$

$$\begin{aligned} \mathcal{G}^\phi = \mathcal{H}^\phi = & \frac{-CH}{864\pi^2 f_\phi^2 \delta} \\ & \times \frac{M_N}{M_T} \mu_N \left[-2(\delta^3 + 3\pi m_\phi^3) \right] \end{aligned}$$

$$\begin{aligned}
 &+ (6\delta^3 - 9\delta m_\phi^2) \ln\left(\frac{m_\phi^2}{\lambda^2}\right) \\
 &+ 12(m_\phi^2 - \delta^2)^{3/2} \arccos\left(\frac{\delta}{m_\phi}\right) \Big], \tag{47}
 \end{aligned}$$

$$\mathcal{I}^\phi = \mathcal{J}^\phi = -\frac{m_\phi^2}{64\pi^2 f_\phi^2} \frac{M_N}{M_T} \ln \frac{m_\phi^2}{\lambda^2} \mu_N M, \tag{48}$$

$$\mathcal{K}^\phi = -\frac{H^2 m_\phi^2}{576\pi^2 f_\phi^2} \left(15 \ln \frac{m_\phi^2}{\lambda^2} + 26\right), \tag{49}$$

$$\begin{aligned}
 \mathcal{L}^\phi = \frac{-C^2}{64\pi^2 f_\phi^2} \Big[&2\delta^2 + (m_\phi^2 - 2\delta^2) \ln \frac{m_\phi^2}{\lambda^2} \\
 &+ 4\delta \sqrt{m_\phi^2 - \delta^2} \arccos\left(\frac{\delta}{m_\phi}\right) \Big]. \tag{50}
 \end{aligned}$$

The γ_{e-h}^ϕ , δ^ϕ , η^ϕ and ξ^ϕ are loop coefficients, which are listed in Table 6.

Apart from the loop diagrams, there is a tree diagram which contributes to the $\mathcal{O}(p^3)$ magnetic moments. The Lagrangian is given in Eq. (36). The contribution reads

$$\mu_{\text{tree}}^{(3)} = -2\phi \frac{M_N}{M_T} \mu_N \tag{51}$$

where the coefficients ϕ are given in Table 7. Up to $\mathcal{O}(p^3)$ magnetic moments, there are 13 LECs, \tilde{g}_A , C , H , $b_{1,2}^{tt,bb,bt}$, g_2^{tt} , and $a_{1,2,3}$.

5 Numerical results and discussions

Since the spin- $\frac{3}{2}$ doubly charmed baryons have not been observed in the experiments, we do not have any experimental inputs to fit the LECs. However, we can employ quark model to determine some of the LECs. The numerical results are given in Table 3.

There are two unknown LECs $b_{1,2}^{tt}$ up to leading order ($\mathcal{O}(p^1)$) magnetic moments. Unlike the light baryons, the charge matrix Q_B of the doubly charmed baryons is not traceless. The heavy quarks contribute to the trace part of the charge matrix. Thus, in the second column of Table 3, the b_1^{tt} terms come from the light quark contribution. The b_2^{tt} terms are the same for the three doubly charmed baryons and arise solely from the two charm quarks.

At the quark level, the flavor and spin wave function of the \mathcal{E}_{cc}^{*++} reads

$$|\mathcal{E}_{cc}^{*++}; S_3 = \frac{3}{2}\rangle = |c \uparrow c \uparrow u \uparrow\rangle, \tag{52}$$

where the arrow denotes the third component of the spin. The magnetic moments of the baryons in the quark model are the matrix elements of the following operator μ sandwiched between the wave functions:

Table 2 The numerical results of spin- $\frac{3}{2}$ doubly heavy baryon magnetic moments from naive quark model estimation. Set A and set B are two constituent quark masses sets from Refs. [47,64], respectively

Baryons	Magnetic moments	Set A	Set B
\mathcal{E}_{cc}^{*++}	$2\mu_c + \mu_u$	2.61	2.45
\mathcal{E}_{cc}^{*+}	$2\mu_c + \mu_d$	-0.18	-0.13
Ω_{cc}^{*+}	$2\mu_c + \mu_s$	0.17	0.15
\mathcal{E}_{bb}^{*0}	$2\mu_b + \mu_u$	1.73	1.60
\mathcal{E}_{bb}^{*-}	$2\mu_b + \mu_d$	-1.06	-0.99
Ω_{bb}^{*-}	$2\mu_b + \mu_s$	-0.71	-0.71
\mathcal{E}_{bc}^{*+}	$\mu_b + \mu_c + \mu_u$	2.17	2.03
\mathcal{E}_{bc}^{*0}	$\mu_b + \mu_c + \mu_d$	-0.62	-0.56
Ω_{bc}^{*0}	$\mu_b + \mu_c + \mu_s$	-0.27	-0.28

$$\mu = \sum_i \mu_i \sigma_3^i, \tag{53}$$

where μ_i is the magnetic moment of the quark;

$$\mu_i = \frac{e_i}{2m_i}, \quad i = u, d, s, c, b. \tag{54}$$

We adopt the constituent quark masses from Ref. [64] as the set A with $m_u = m_d = 336$ MeV, $m_s = 540$ MeV, $m_c = 1660$ MeV and $m_b = 4700$ MeV. We adopt the constituent quark masses from Ref. [47] as the set B with $m_u = m_d = 363$ MeV, $m_s = 538$ MeV, $m_c = 1711$ MeV and $m_b = 5044$ MeV. The magnetic moments from the naive quark model estimation with set A and B are given in Table 2. The two sets lead to the similar magnetic moments. We choose the results of set A in the following calculation.

The $\mathcal{O}(p^1)$ magnetic moments of the spin- $\frac{3}{2}$ doubly charmed baryons are given in the second column in Table 3. The numerical results from the quark model are given in the third column. In the quark model, the light quark parts contribute to the b_1^{tt} terms, which are proportional to the light quark charge. The heavy quark parts contribute to the b_2^{tt} terms, which are the same for the three doubly charmed baryons.

Up to $\mathcal{O}(p^2)$, we must take the loop corrections into consideration. At this order, there exist three new LECs \tilde{g}_A , C and H , which are estimated in the quark model [76,90]. The numerical results are given in the third column of Table 3.

In Table 3, the magnetic moments of the \mathcal{E}_{cc}^{*++} and \mathcal{E}_{cc}^{*+} are dominated by the leading order term while the magnetic moment of Ω_{cc}^{*+} is dominated by the chiral corrections. At the leading order, since three quarks in \mathcal{E}_{cc}^{*++} all have the positive charge, their contributions to the magnetic moments are constructive. For the \mathcal{E}_{cc}^{*+} and Ω_{cc}^{*+} , the contribution of the heavy quarks and light quark cancel out to a large

Table 3 The spin- $\frac{3}{2}$ doubly charmed baryon magnetic moments when the chiral expansion is truncated at $\mathcal{O}(p^1)$ and $\mathcal{O}(p^2)$, respectively (in

unit of μ_N). The magnetic moments in the third column are evaluated by quark model, which are treated as the $\mathcal{O}(p^1)$ magnetic moments. We adopt $\delta = -100$ MeV and $\delta = -70$ MeV as two parameter sets

Baryons	$\mathcal{O}(p^1)$	Quark model	δ (MeV)	$\mathcal{O}(p^2)$ I	Total I	δ (MeV)	$\mathcal{O}(p^2)$ II	Total II
Ξ_{cc}^{*++}	$-\frac{4}{3}\frac{M_N}{M_T}b_1^{II} - \frac{8}{3}\frac{M_N}{M_T}b_2^{II}$	$2\mu_c + \mu_u = 2.61$	- 100	0.90	3.51	- 70	1.02	3.63
Ξ_{cc}^{*+}	$\frac{2}{3}\frac{M_N}{M_T}b_1^{II} - \frac{8}{3}\frac{M_N}{M_T}b_2^{II}$	$2\mu_c + \mu_d = -0.18$	- 100	- 0.09	- 0.27	- 70	- 0.19	- 0.37
Ω_{cc}^{*+}	$\frac{2}{3}\frac{M_N}{M_T}b_1^{II} - \frac{8}{3}\frac{M_N}{M_T}b_2^{II}$	$2\mu_c + \mu_s = 0.17$	- 100	- 0.81	- 0.64	- 70	- 0.82	- 0.65

Table 4 The spin- $\frac{3}{2}$ doubly bottom baryon (bbq) and charmed bottom baryon (bcq) magnetic moments to the next-to-leading order (in unit of μ_N). We use the subscripts bc to label the systems with symmetric

spin wave functions in the heavy quark sector. We adopt $\delta = -40$ and $\delta = -20$ MeV for the doubly bottom baryons and $\delta = -60$ and $\delta = -20$ MeV for the charmed bottom baryons

Baryons	$\mathcal{O}(p^1)$	δ (MeV)	$\mathcal{O}(p^2)$ I	Total I	δ (MeV)	$\mathcal{O}(p^2)$ II	Total II
Ξ_{bb}^{*0}	$2\mu_b + \mu_u = 1.73$	- 40	1.10	2.83	- 20	1.15	2.87
Ξ_{bb}^{*-}	$2\mu_b + \mu_d = -1.06$	- 40	- 0.27	- 1.33	- 20	- 0.31	- 1.38
Ω_{bb}^{*-}	$2\mu_b + \mu_s = -0.71$	- 40	- 0.83	- 1.54	- 20	- 0.83	- 1.55
Ξ_{bc}^{*+}	$\mu_b + \mu_c + \mu_u = 2.17$	- 60	1.05	3.22	- 40	1.10	3.27
Ξ_{bc}^{*0}	$\mu_b + \mu_c + \mu_d = -0.62$	- 60	- 0.22	- 0.84	- 40	- 0.27	- 0.89
Ω_{bc}^{*0}	$\mu_b + \mu_c + \mu_s = -0.27$	- 60	- 0.82	- 1.09	- 40	- 0.83	- 1.10

extent, which leads to small magnetic moments at the leading order.

At the next-to-leading order, both π^+ and K^+ mesons contribute to the chiral correction of $\mu_{\Xi_{cc}^{*++}}$, while only π^+ (K^+) contributes to $\mu_{\Xi_{cc}^{*+}}$ ($\mu_{\Omega_{cc}^{*+}}$). The chiral corrections in the loops (a) and (b) are proportional to the pseudoscalar meson mass, i.e., $\sim \frac{m_\phi}{M_T}$. Therefore, the chiral corrections for $\mu_{\Xi_{cc}^{*++}}$ and $\mu_{\Omega_{cc}^{*+}}$ are much larger than that for $\mu_{\Xi_{cc}^{*+}}$. It is interesting to note that the chiral correction from the K^+ loop for the $\mu_{\Omega_{cc}^{*+}}$ is much larger than the leading order contribution. Such a unique feature might be exposed by future lattice QCD simulation.

Up to $\mathcal{O}(p^3)$, eight new LECs, $b_{1,2}^{bb,bt}$, g_2^{tt} and $a_{1,2,3}$ are introduced. Since it is impossible to fix all these LECs due to lack of experimental data, we do not present the numerical results up to this order.

With the same formalism, we have also calculated the magnetic moments of the doubly bottom baryons and charmed bottom baryons. Since the b quark is much heavier than the c quark, we adopt the mass splitting $\delta = -40$ MeV and $\delta = -20$ MeV for the doubly bottom baryons and $\delta = -60$ MeV and $\delta = -40$ MeV for the charmed bottom baryons. The above mass difference in our work is consistent with that in Refs. [35,39,47,51]. The leading order magnetic moments and the LECs in the next-to-leading order magnetic moments are estimated by the quark model. We present the numerical results of the doubly bottom baryon and charmed bottom baryons magnetic moments to next-to-leading order in Table 4.

6 Conclusions

The doubly heavy baryons are particularly interesting because their chiral dynamics is solely dominated by the single light quark. In this work, we have employed the heavy baryon chiral perturbation theory to calculate the magnetic moments of the spin- $\frac{3}{2}$ doubly charmed baryons, which reveal the information of their inner structure. Due to the large mass of the doubly heavy baryons, the recoil corrections are expected to be very small. We have derived our analytical expressions up to the next-to-next-to-leading order, which may be useful to the possible chiral extrapolation of the lattice simulations of the doubly charmed baryon electromagnetic properties.

With the help of the quark model, we have estimated the LECs and presented the numerical results up to next-to-leading order: $\mu_{\Xi_{cc}^{*++}} = 3.51\mu_N$, $\mu_{\Xi_{cc}^{*+}} = -0.27\mu_N$, $\mu_{\Omega_{cc}^{*+}} = -0.64\mu_N$ for $\delta = -100$ MeV and $\mu_{\Xi_{cc}^{*++}} = 3.63\mu_N$, $\mu_{\Xi_{cc}^{*+}} = -0.37\mu_N$, $\mu_{\Omega_{cc}^{*+}} = -0.65\mu_N$ for $\delta = -70$ MeV. As by-products, we have also calculated the magnetic moments of the spin- $\frac{3}{2}$ doubly bottom baryons and charmed bottom baryons.

For comparison, we have listed the spin- $\frac{3}{2}$ doubly charmed baryon magnetic moments from some other model calculations in Table 5 including the quark model [64], MIT bag model [70,71], skyrmion model [73], non-relativistic quark model (NRQM) [34], hyper central quark model (HCQM) [39], effective mass and screened charge scheme [67] and chiral constituent quark model (χ CQM) [69]. We define the relative changes ρ of these models with respect to the naive estimates as $\mu = (1 + \rho)\mu_{QM}$, where μ_{QM} is the

Table 5 Comparison of the spin- $\frac{3}{2}$ doubly charmed baryons magnetic moments in the literature including the quark model [64], MIT bag model [70,71], skyrmion model [73], non-relativistic quark model (NRQM) [34], hyper central model (HCQM) [39], effective mass and screened charge scheme [67]. We adopt $\delta = -100$ MeV and $\delta = -70$ MeV as I and II parameter sets, respectively, in this work

	\mathcal{E}_{cc}^{*++}	\mathcal{E}_{cc}^{*+}	Ω_{cc}^{*+}
Quark model [64]	2.60	-0.19	0.17
Bag model 1 [70]	2.54	0.20	0.39
Bag model 2 [71]	2.00	0.16	0.33
Skyrmion 1 [73]	3.16	-0.98	-0.20
Skyrmion 2 [73]	3.18	-1.17	0.03
NRQM [34]	2.67	-0.31	0.14
HCQM [39]	2.75	-0.17	0.12
Effective mass [67]	2.41	-0.11	0.16
Screened charge [67]	2.52	0.04	0.21
χ CQM [69]	2.66	-0.47	0.14
This work I	3.51	-0.27	-0.64
This work II	3.63	-0.37	-0.65

magnetic moments estimated with the naive quark model. For the \mathcal{E}_{cc}^{*++} baryon, one notices that $|\rho| < 0.1$ for most models, and $|\rho| < 0.4$ for all models. Thus, all these approaches lead to more or less similar numerical results for the magnetic moments of \mathcal{E}_{cc}^{*++} . For the \mathcal{E}_{cc}^{*+} baryon, $|\rho| < 2.5$ for most models, including our work, while $|\rho| > 4$ from the skyrmion models. For the Ω_{cc}^{*+} baryon, the $|\rho| < 2$ in all the models except our work and one skyrmion calculation. Thus, various models lead to quite different predictions for the magnetic moments of \mathcal{E}_{cc}^{*+} and Ω_{cc}^{*+} , which may be used to distinguish these models.

In our calculation, the value for $\mu_{\Omega_{cc}^{*+}}$ is negative, which is different from other model predictions. The chiral correction from the kaon loop is large and negative, which dominates the leading order term estimated from the quark model. Therefore, the HBChPT formalism predicts a negative value for $\mu_{\Omega_{cc}^{*+}}$ up to $\mathcal{O}(p^2)$.

In the numerical analysis, we have truncated the chiral expansions at $\mathcal{O}(p^2)$ and omitted all the $\mathcal{O}(p^3)$ higher order chiral corrections because of too many unknown LECs at this order. When more experimental measurements become

available in the future, the numerical analysis in the present work can be further improved. In principle, all the low energy constants shall be extracted through fitting to the experimental data instead of using the estimation from the quark model. The $\mathcal{O}(p^3)$ chiral corrections may turn out to be non-negligible and should be included.

There is good hope that the spin- $\frac{3}{2}$ doubly charmed baryons will be observed through its radiative or weak decays in the coming future. We hope our numerical calculation may be useful for future experimental measurements of their magnetic moments. There are several LECs in our analytical results to be determined by the future progress in experiment and theory, which will help check the chiral expansion convergence of the three doubly charmed baryons.

Acknowledgements L. Meng is very grateful to X. L. Chen and W. Z. Deng for very helpful discussions. This project is supported by the National Natural Science Foundation of China under Grants 11575008, 11621131001 and 973 program. This work is also supported by the Fundamental Research Funds for the Central Universities of Lanzhou University under Grants 223000-862637.

Open Access This article is distributed under the terms of the Creative Commons Attribution 4.0 International License (<http://creativecommons.org/licenses/by/4.0/>), which permits unrestricted use, distribution, and reproduction in any medium, provided you give appropriate credit to the original author(s) and the source, provide a link to the Creative Commons license, and indicate if changes were made. Funded by SCOAP³.

Appendix A: Coefficients of the loop corrections

In this appendix, we collect the explicit formulas for the chiral expansion of the doubly charmed baryon magnetic moments in Tables 6 and 7.

Table 7 The coefficients of the tree diagrams in Fig. 1, which contribute to the $\mathcal{O}(p^1)$ and $\mathcal{O}(p^3)$ magnetic moments

α	ϕ		
\mathcal{E}_{cc}^{*++}	$\frac{2}{3}b_1'' + \frac{4}{3}b_2''$	$-\frac{4}{9}a_1 - \frac{1}{9}a_2 - \frac{4}{9}a_3$	
\mathcal{E}_{cc}^{*+}	$-\frac{1}{3}b_1'' + \frac{4}{3}b_2''$	$-\frac{4}{9}a_1 - \frac{1}{9}a_2 + \frac{2}{9}a_3$	
Ω_{cc}^{*+}	$-\frac{1}{3}b_1'' + \frac{4}{3}b_2''$	$\frac{8}{9}a_1 - \frac{1}{9}a_2 - \frac{4}{9}a_3$	

Table 6 The coefficients of the loop corrections to the spin- $\frac{3}{2}$ doubly charmed baryon magnetic moments from Fig. 2. For diagrams (e)–(h), the LECs $b_{1,2}$ in the table represent $b_{1,2}^{\pi\pi}, b_{1,2}^{\pi K}, b_{1,2}^{\pi\eta}$ and $b_{1,2}^{\eta\eta}$ in order

	β_a^π	β_a^K	γ_{e-h}^π	γ_{e-h}^K	γ_{e-h}^η	δ^π	δ^K	η^π	η^K	ξ^π	ξ^K	ξ^η
\mathcal{E}_{cc}^{*++}	-4	-4	$4b_2$	$\frac{2}{3}(-b_1 + 4b_2)$	$\frac{2}{9}(b_1 + 2b_2)$	$-4b_1''$	$-4b_1''$	$-8g_2''$	$-8g_2''$	3	2	$\frac{1}{3}$
\mathcal{E}_{cc}^{*+}	4		$b_1 + 4b_2$	$\frac{2}{3}(-b_1 + 4b_2)$	$\frac{1}{9}(-b_1 + 4b_2)$	$4b_1''$		$8g_2''$		3	2	$\frac{1}{3}$
Ω_{cc}^{*+}		4		$\frac{2}{3}(b_1 + 8b_2)$	$\frac{4}{9}(-b_1 + 4b_2)$		$4b_1''$		$8g_2''$		4	$\frac{4}{3}$

References

1. M. Mattson et al., SELEX Collaboration, Phys. Rev. Lett. **89**, 112001 (2002)
2. S.P. Ratti, Nucl. Phys. Proc. Suppl. **115**, 33 (2003)
3. B. Aubert et al., BaBar Collaboration, Phys. Rev. D **74**, 011103 (2006)
4. R. Chistov et al., Belle Collaboration, Phys. Rev. Lett. **97**, 162001 (2006)
5. R. Aaij et al., LHCb Collaboration, Phys. Rev. Lett. **119**(11), 112001 (2017)
6. C.H. Chang, C.F. Qiao, J.X. Wang, X.G. Wu, Phys. Rev. D **73**, 094022 (2006)
7. C.H. Chang, J.P. Ma, C.F. Qiao, X.G. Wu, J. Phys. G **34**, 845 (2007)
8. C.H. Chang, T. Li, X.Q. Li, Y.M. Wang, Commun. Theor. Phys. **49**, 993 (2008)
9. C.H. Chang, J.X. Wang, X.G. Wu, Comput. Phys. Commun. **177**, 467 (2007)
10. C.H. Chang, J.X. Wang, X.G. Wu, Comput. Phys. Commun. **181**, 1144 (2010)
11. X.C. Zheng, C.H. Chang, Z. Pan, Phys. Rev. D **93**(3), 034019 (2016)
12. G. Chen, X.G. Wu, Z. Sun, Y. Ma, H.B. Fu, JHEP **1412**, 018 (2014)
13. G. Chen, X.G. Wu, J.W. Zhang, H.Y. Han, H.B. Fu, Phys. Rev. D **89**(7), 074020 (2014)
14. H.Y. Bi, R.Y. Zhang, X.G. Wu, W.G. Ma, X.Z. Li, S. Owusu, Phys. Rev. D **95**(7), 074020 (2017)
15. E. Bagan, M. Chabab, S. Narison, Phys. Lett. B **306**, 350 (1993)
16. R. Roncaglia, D.B. Lichtenberg, E. Predazzi, Phys. Rev. D **52**, 1722 (1995)
17. B. Silvestre-Brac, Few Body Syst. **20**, 1 (1996)
18. D. Ebert, R.N. Faustov, V.O. Galkin, A.P. Martynenko, V.A. Saleev, Z. Phys. C **76**, 111 (1997)
19. S.P. Tong, Y.B. Ding, X.H. Guo, H.Y. Jin, X.Q. Li, P.N. Shen, R. Zhang, Phys. Rev. D **62**, 054024 (2000)
20. C. Itoh, T. Minamikawa, K. Miura, T. Watanabe, Phys. Rev. D **61**, 057502 (2000)
21. S.S. Gershtein, V.V. Kiselev, A.K. Likhoded, A.I. Onishchenko, Phys. Rev. D **62**, 054021 (2000)
22. V.V. Kiselev, A.K. Likhoded, Phys. Usp. **45**, 455 (2002)
23. V.V. Kiselev, A.K. Likhoded, Usp. Fiz. Nauk. **172**, 497 (2002)
24. V.V. Kiselev, A.K. Likhoded, O.N. Pakhomova, V.A. Saleev, Phys. Rev. D **66**, 034030 (2002)
25. I.M. Narodetskii, M.A. Trusov, Phys. Atom. Nucl. **65**, 917 (2002)
26. I.M. Narodetskii, M.A. Trusov, Yad. Fiz. **65**, 949 (2002)
27. R. Lewis, N. Mathur, R.M. Woloshyn, Phys. Rev. D **64**, 094509 (2001)
28. D. Ebert, R.N. Faustov, V.O. Galkin, A.P. Martynenko, Phys. Rev. D **66**, 014008 (2002)
29. N. Mathur, R. Lewis, R.M. Woloshyn, Phys. Rev. D **66**, 014502 (2002)
30. J.M. Flynn et al., UKQCD Collaboration, JHEP **0307**, 066 (2003)
31. J. Vijande, H. Garcilazo, A. Valcarce, F. Fernandez, Phys. Rev. D **70**, 054022 (2004)
32. T.W. Chiu, T.H. Hsieh, Nucl. Phys. A **755**, 471 (2005)
33. S. Migura, D. Merten, B. Metsch, H.R. Petry, Eur. Phys. J. A **28**, 41 (2006)
34. C. Albertus, E. Hernandez, J. Nieves and J. M. Verde-Velasco, Eur. Phys. J. A **32**, 183 (2007) [Erratum: Eur. Phys. J. A **36**, 119 (2008)]
35. A.P. Martynenko, Phys. Lett. B **663**, 317 (2008)
36. L. Tang, X.H. Yuan, C.F. Qiao, X.Q. Li, Commun. Theor. Phys. **57**, 435 (2012)
37. X. Liu, H.X. Chen, Y.R. Liu, A. Hosaka, S.L. Zhu, Phys. Rev. D **77**, 014031 (2008)
38. W. Roberts, M. Pervin, Int. J. Mod. Phys. A **23**, 2817 (2008)
39. B. Patel, A. K. Rai, P. C. Vinodkumar, J. Phys. G **35**, 065001 (2008). [arXiv:0803.0221](https://arxiv.org/abs/0803.0221) [hep-ph]. [J. Phys. Conf. Ser. **110**, 122010 (2008)]
40. A. Valcarce, H. Garcilazo, J. Vijande, Eur. Phys. J. A **37**, 217 (2008)
41. L. Liu, H.W. Lin, K. Orginos, A. Walker-Loud, Phys. Rev. D **81**, 094505 (2010)
42. Y. Namekawa, PACS-CS Collaboration, PoS LATTICE **2012**, 139 (2012)
43. C. Alexandrou, J. Carbonell, D. Christaras, V. Drach, M. Gravina, M. Papinutto, Phys. Rev. D **86**, 114501 (2012)
44. T.M. Aliev, K. Azizi, M. Savci, Nucl. Phys. A **895**, 59 (2012)
45. T.M. Aliev, K. Azizi, M. Savci, J. Phys. G **40**, 065003 (2013)
46. Y. Namekawa et al., PACS-CS Collaboration, Phys. Rev. D **87**(9), 094512 (2013)
47. M. Karliner, J.L. Rosner, Phys. Rev. D **90**(9), 094007 (2014)
48. Z.F. Sun, Z.W. Liu, X. Liu, S.L. Zhu, Phys. Rev. D **91**(9), 094030 (2015)
49. H.X. Chen, W. Chen, Q. Mao, A. Hosaka, X. Liu, S.L. Zhu, Phys. Rev. D **91**(5), 054034 (2015)
50. Z.F. Sun, M.J. Vicente Vacas, Phys. Rev. D **93**(9), 094002 (2016)
51. Z. Shah, K. Thakkar, A.K. Rai, Eur. Phys. J. C **76**(10), 530 (2016)
52. H.X. Chen, W. Chen, X. Liu, Y.R. Liu, S.L. Zhu, Rep. Prog. Phys. **80**(7), 076201 (2017)
53. A. V. Kiselev, A. V. Berezhnoy A. K. Likhoded, [arXiv:1706.09181](https://arxiv.org/abs/1706.09181) [hep-ph]
54. H.X. Chen, Q. Mao, W. Chen, X. Liu, S.L. Zhu, Phys. Rev. D **96**(3), 031501 (2017)
55. J. Hu, T. Mehen, Phys. Rev. D **73**, 054003 (2006)
56. F. S. Yu, H. Y. Jiang, R. H. Li, C. D. Lü, W. Wang, Z. X. Zhao, [arXiv:1703.09086](https://arxiv.org/abs/1703.09086) [hep-ph]
57. R.H. Li, C.D. Lü, W. Wang, F.S. Yu, Z.T. Zou, Phys. Lett. B **767**, 232 (2017)
58. L. Meng, N. Li, S.L. Zhu, Phys. Rev. D **95**(11), 114019 (2017). [arXiv:1707.03598](https://arxiv.org/abs/1707.03598) [hep-ph]
59. Z.H. Guo, Phys. Rev. D **96**(7), 074004 (2017)
60. W. Wang, F. S. Yu, Z. X. Zhao, [arXiv:1707.02834](https://arxiv.org/abs/1707.02834) [hep-ph]. <https://doi.org/10.1140/epjc/s10052-017-5360-1>
61. W. Wang, Z. P. Xing, J. Xu, [arXiv:1707.06570](https://arxiv.org/abs/1707.06570) [hep-ph]. <https://doi.org/10.1140/epjc/s10052-017-5363-y>
62. Q. F. Lü, K. L. Wang, L. Y. Xiao, X. H. Zhong, [arXiv:1708.04468](https://arxiv.org/abs/1708.04468) [hep-ph]. <https://doi.org/10.1103/PhysRevD.96.114006>
63. L. Y. Xiao, K. L. Wang, Q. F. Lu, X. H. Zhong, S. L. Zhu, [arXiv:1708.04384](https://arxiv.org/abs/1708.04384) [hep-ph]. <https://doi.org/10.1103/PhysRevD.96.094005>
64. D.B. Lichtenberg, Phys. Rev. D **15**, 345 (1977)
65. B. Julia-Diaz, D.O. Riska, Nucl. Phys. A **739**, 69 (2004)
66. A. Faessler, T. Gutsche, M.A. Ivanov, J.G. Korner, V.E. Lyubovitskij, D. Nicmorus, K. Pumsa-ard, Phys. Rev. D **73**, 094013 (2006)
67. R. Dhir, R.C. Verma, Eur. Phys. J. A **42**, 243 (2009)
68. T. Branz, A. Faessler, T. Gutsche, M.A. Ivanov, J.G. Korner, V.E. Lyubovitskij, B. Oexl, Phys. Rev. D **81**, 114036 (2010)
69. N. Sharma, H. Dahiya, P.K. Chatley, M. Gupta, Phys. Rev. D **81**, 073001 (2010)
70. S.K. Bose, L.P. Singh, Phys. Rev. D **22**, 773 (1980)
71. A. Bernotas, V. Simonis, [arXiv:1209.2900](https://arxiv.org/abs/1209.2900) [hep-ph]
72. S.N. Jena, D.P. Rath, Phys. Rev. D **34**, 196 (1986)
73. Y.S. Oh, D.P. Min, M. Rho, N.N. Scoccola, Nucl. Phys. A **534**, 493 (1991)
74. K.U. Can, G. Erkol, B. Isildak, M. Oka, T.T. Takahashi, Phys. Lett. B **726**, 703 (2013)
75. K.U. Can, G. Erkol, B. Isildak, M. Oka, T.T. Takahashi, JHEP **1405**, 125 (2014)
76. H. S. Li, L. Meng, Z. W. Liu, S. L. Zhu, [arXiv:1707.02765](https://arxiv.org/abs/1707.02765) [hep-ph]. <https://doi.org/10.1103/PhysRevD.96.076011>
77. S. Weinberg, Physica A **96**, 327 (1979)
78. S. Scherer, Adv. Nucl. Phys. **27**, 277 (2003)
79. E.E. Jenkins, A.V. Manohar, Phys. Lett. B **255**, 558 (1991)

80. E. E. Jenkins, M. E. Luke, A. V. Manohar, M. J. Savage, *Phys. Lett. B* **302**, 482 (1993) [Erratum: *Phys. Lett. B* **388**, 866 (1996)]
81. V. Bernard, N. Kaiser, J. Kambor, U.G. Meissner, *Nucl. Phys. B* **388**, 315 (1992)
82. V. Bernard, N. Kaiser, U.G. Meissner, *Int. J. Mod. Phys. E* **4**, 193 (1995)
83. U.G. Meissner, S. Steininger, *Nucl. Phys. B* **499**, 349 (1997)
84. H.S. Li, Z.W. Liu, X.L. Chen, W.Z. Deng, S.L. Zhu, *Phys. Rev. D* **95**(7), 076001 (2017)
85. T.R. Hemmert, B.R. Holstein, J. Kambor, *Phys. Lett. B* **395**, 89 (1997)
86. T.R. Hemmert, B.R. Holstein, J. Kambor, *J. Phys. G* **24**, 1831 (1998)
87. G.C. Gellas, T.R. Hemmert, C.N. Ktorides, G.I. Poulis, *Phys. Rev. D* **60**, 054022 (1999)
88. T.A. Gail, T.R. Hemmert, *Eur. Phys. J. A* **28**, 91 (2006)
89. H. S. Li, Z. W. Liu, X. L. Chen, W. Z. Deng, S. L. Zhu, [arXiv:1706.06458](https://arxiv.org/abs/1706.06458) [hep-ph]
90. H. S. Li, L. Meng, Z. W. Liu, S. L. Zhu, [arXiv:1708.03620](https://arxiv.org/abs/1708.03620) [hep-ph]
91. S. Nozawa, D.B. Leinweber, *Phys. Rev. D* **42**, 3567 (1990)
92. W. Rarita, J. Schwinger, *Phys. Rev.* **60**, 61 (1941)
93. G. Ecker, *Prog. Part. Nucl. Phys.* **35**, 1 (1995)
94. U. G. Meissner, [arXiv:hep-ph/9711365](https://arxiv.org/abs/hep-ph/9711365)